

Magnetic-field-induced superelasticity of ferromagnetic thermoelastic martensites: Experiment and modeling

V. A. Chernenko

Institute of Magnetism, Vernadsky str. 36-b, Kyiv 03142, Ukraine

V. A. L'vov

Radiophysics Department, Taras Shevchenko University, Kyiv 03127, Ukraine

P. Müllner and G. Kostorz

ETH Zürich, Institute of Applied Physics, CH-8093 Zürich, Switzerland

T. Takagi*

Institute of Fluid Science, Tohoku University, Sendai 980-8577, Japan

(Received 11 August 2003; revised manuscript received 20 November 2003; published 6 April 2004)

The superelastic effect under constant magnetic fields exhibited by the Ni-Mn-Ga ferromagnetic thermoelastic martensites with single-variant and polyvariant microstructure is studied experimentally and theoretically. The formerly proposed statistical model of the magnetostrain effect in the ferromagnetic martensite is modified for the theoretical description of the superelastic stress-strain dependence under magnetic field. The mechanical stress, which is equivalent to the internal stress induced by the magnetic field, is determined by fitting the theoretical stress-strain curves to the experimental results. A quadratic dependence of the field-induced stress on the value of the magnetization of martensite is found. This dependence supports the model assumption that a magnetoelastic interaction causes the magnetostrain effect.

DOI: 10.1103/PhysRevB.69.134410

PACS number(s): 75.50.-y, 75.80.+q

I. INTRODUCTION

Ferromagnetic thermoelastic martensites, such as those formed in $\text{Ni}_{2+x+y}\text{Mn}_{1-x}\text{Ga}_{1-y}$ Heusler alloys,¹ exhibit a large strain upon application of a magnetic field.²⁻⁴ The ferromagnetic thermoelastic martensites are characterized by spatially inhomogeneous magnetic ordering coupled to highly mobile twin boundaries by magnetoelastic interactions.⁵ Very-low-yield stresses,^{4,6,7} mechanically driven change of magnetization,⁸ reversible and irreversible strains induced by magnetic fields (magnetoelasticity and magnetoplasticity, respectively),^{2-4,6,9} and a magnetic-field-induced increase of the yield stress (magnetostress) (Ref. 10) have been observed and are the subject of current research.

Theoretical studies of the phenomena exhibited by the ferromagnetic thermoelastic martensites are numerous.^{4,5,11-18} The essential features of the magnetic¹⁸ and magnetoelastic behavior of ferromagnetic martensites were quantitatively described in the framework of a magnetoelastic model.^{5,13-15} According to the model, magnetoelasticity and magnetoplasticity are caused by spin-lattice interactions in solids containing magnetic atoms. For comprehension of the magnetoelastic behavior of ferromagnetic martensites, the concept of magnetic-field-induced stress was proposed and an equivalence principle was substantiated thermodynamically for the field-induced and mechanical stresses.¹³⁻¹⁵ The theoretical value of the conversion coefficient from magnetic field to mechanical stress estimated from the magnetoelastic model proved to be in good agreement with the experimental value.¹⁶

The nonlinear irreversible field dependences of both magnetoplastic strain (i.e., strain caused by the irreversible mo-

tion of twinning dislocations) (Ref. 4) and magnetization of martensite were successfully analyzed using a statistical distribution of the energy barriers separating the metastable arrangements of martensitic twins.^{16,17} Thus, a statistical approach based on the equivalence principle between magnetostress and mechanical stress turned out to be a powerful tool to tackle the whole spectrum of problems related to the magnetomechanics of ferromagnetic martensites.

In the present paper, the statistical approach is modified for a description of the stress-strain characteristics of martensites affected by a constant magnetic field. A procedure for the determination of the magnetic-field-induced stress is proposed and applied to the results obtained for a single-crystalline specimen of $\text{Ni}_{52.0}\text{Mn}_{24.4}\text{Ga}_{23.6}$ consisting of only one martensite domain with two twin variants. The procedure is based on a fitting of loops computed using the statistical model to the experimental stress-strain loops taken in the presence of a constant magnetic field. The data clearly show a *quadratic dependence of the field-induced stress on the magnetization of the alloy*. This dependence substantiates the magnetoelastic model of ferromagnetic martensite. Experimental superelastic loops measured for a second single crystal containing many martensite and twin variants are also analyzed, and applicability of the statistical model to more complicated twin structures is demonstrated.

II. EXPERIMENT

Single-crystalline $\text{Ni}_{52.0}\text{Mn}_{24.4}\text{Ga}_{23.6}$ alloy (denoted as NMG1) and $\text{Ni}_{51.0}\text{Mn}_{28.0}\text{Ga}_{21.0}$ alloy (NMG2) were grown with the Bridgman method using ingots prepared from the elements by induction melting in vacuum. The characteristic

temperatures $T_M=307$ K, $T_A=313$ K, and $T_C=361$ K for NMG1 and $T_M=314$ K, $T_A=316$ K, and $T_C=370$ K for NMG2 (T_M and T_A are the forward and reverse martensitic transformation temperatures and T_C is the Curie temperature) were obtained from measurements of the temperature dependence of the low-field magnetic susceptibility. Electron diffraction at room temperature revealed a five-layer modulated tetragonal structure of the martensitic phase with $c/a=0.94$ for both alloys (c and a denote the values of the lattice parameters). Parallelepiped-shaped samples with all faces parallel to $\{100\}$ of austenite were prepared for magnetomechanical testing. The specimen dimensions were $4.8 \times 3.4 \times 3.3$ mm³ (NMG1) and $5.4 \times 3.2 \times 2.3$ mm³ (NMG2). The parallelism of all faces was better than 10 μ m.

Uniaxial compression tests under an orthogonal magnetic field were done at a constant crosshead speed of 2×10^{-6} m/s in a mechanical testing machine (Zwick, Ulm) equipped with a 500-N load cell (MTS, Schaffhausen) and extensometers insensitive to magnetic fields (Heidenhain, Traunreut). The resolutions were better than 0.5 N in force and 10 nm in displacement. The corresponding uncertainties were 0.1 MPa for stress and 2×10^{-6} for strain. Since the strain magnitude corresponding to the plateaulike region on the stress-strain curves for the NMG1 specimen is equal to the lattice strain (about 6%), NMG1 martensite is qualified as consisting of only one martensite domain, while the microstructure of NMG2 consisted of many different martensite variants.⁸ The magnetic field was produced by a permanent-magnet system (Magnetic Solutions, Dublin) with better than 1% homogeneity at the position of the sample for field strength H and better than 1° for field direction for any arbitrary direction within the plane perpendicular to the load direction. The sample was mounted in such a way that the longest edge was parallel to the mechanical load direction (y direction). The x direction was defined parallel to the shortest edge of the sample, and x - y - z constitute Cartesian coordinates. The field direction was constant and parallel to the shortest edge of the sample (i.e., parallel to the x direction). The sample was mechanically loaded up to 10 MPa and unloaded at constant field strength starting with 2 T, followed by 1.6, 1.4, 1.2, 1.0, 0.9, ..., 0.1, and 0 T. The unloading process was stopped at some minimal force (2 N) which was needed to keep the sample in place. Then, the field was increased to 2 T. During this process, the compressive force increased by a few N. The sample was unloaded again down to 2 N, this time in a field of 2 T. Thereafter, the magnetic field was reduced to the value for the next compression test. The second unloading (with 2 T) was performed to reset the initial state of the specimen.

The room-temperature magnetization curve was measured on a specimen cut from the same single crystal as NMG1 (dimensions were $6.5 \times 1.0 \times 1.9$ mm³; all faces were parallel to $\{100\}$) using a vibrating sample magnetometer VSM-5-18 (Toei Industry Co.). An initial magnetic state of the specimen was set by aligning its long axis along the saturating field.

III. THEORETICAL MODEL

The microstructure of tetragonal NMG1 martensite can be modeled by alternating (101) twin variants, the c axis being

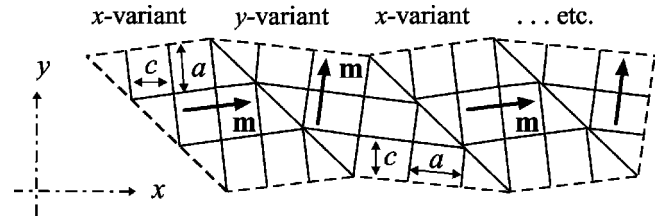


FIG. 1. Schematic presentation of the xy domain in NMG1 ferromagnetic martensite.

aligned with the x and y axes; see Fig. 1. This microstructure is referred to as the xy domain.

The following assumptions are made for describing the deformation of a martensite with $c/a < 1$ consisting of a single xy domain.^{16,17}

(i) The reorientation of martensite variants is caused by the total effective stress $\sigma^{\text{eff}} = \sigma_{xx} - \sigma_{yy}$ which is the sum of mechanical and magnetic-field-induced stresses. It should be noted that σ^{eff} is a scalar quantity representing a normal stress (tensile if positive, compressive if negative) in the x direction acting in each twin variant. The effective stress σ^{eff} is increased if the sample is uniaxially stressed in tension in the x direction or in compression in the y direction.

(ii) The rearrangement of twin boundaries in the xy domain under the action of increasing stress $\sigma^{\text{eff}} > 0$ occurs in two stages. First a small (quasi)reversible displacement of the twin boundary takes place. Then the twin boundary moves at high speed across a full twin and merges with the neighboring boundary. Thereby, twin variants with the c axis parallel to the x direction (x variants) disappear and the c axis (short axis) is progressively more preferred along the y direction until the whole domain is a single y variant.

(iii) The critical stress value σ_n^{eff} (n refers to a specific twin boundary) initiating the rapid motion of the n th twin boundary varies across the sample.

(iv) The critical stress values are statistically distributed around a certain average value σ_c with a probability density p_n (characterizing the rate of the disappearance of one type of the twin variants) which has a normal Gaussian form

$$p_n = \frac{1}{Z} \exp \left\{ - \frac{(|\sigma_n^{\text{eff}}| - |\sigma_c|)^2}{2\sigma_0^2} \right\},$$

$$Z = \sum_n \exp \left\{ - \frac{(|\sigma_n^{\text{eff}}| - |\sigma_c|)^2}{2\sigma_0^2} \right\}, \quad (1)$$

where σ_0 is a constant parameter describing the width of the distribution and Z is the statistical sum.

For each field value the number N of disappeared twins (boundaries jumps) can be found from the condition $|\sigma^{\text{eff}}| \geq |\sigma_n^{\text{eff}}|$. This condition results in the expression

$$N(\sigma^{\text{eff}}) = N_0 \sum_n p_n \theta(|\sigma^{\text{eff}}| - |\sigma_n^{\text{eff}}|), \quad (2)$$

where N_0 is the number of twins in the unstressed specimen in the absence of a magnetic field and θ is the Heaviside function, which is introduced to account for condition (ii).

According to assumption (i), the values σ^{eff} and N are functions of the components of the mechanical stress tensor σ_{ik} and the magnetic field H_j :

$$\sigma^{\text{eff}} = \sigma^{\text{eff}}(\sigma_{ik}, H_j), \quad N = N(\sigma_{ik}, H_j). \quad (3)$$

A statistical model based on assumptions (i)–(iv) and Eq. (2) is developed elsewhere.¹⁷ According to this model, the volume fraction α_y of y variant in the xy domain affected by the stationary field $\mathbf{H} \parallel x$ and an increasing mechanical stress σ_{yy} (forward stress path) is given by

$$\alpha_y(\sigma_{yy}, H) = \begin{cases} \alpha_y(0, H)[1 - N(\sigma_{yy}, H)/N_0], & \sigma^{\text{eff}} < 0, \\ \alpha_y(0, H) + [1 - \alpha_y(0, H)]N(\sigma_{yy}, H)/N_0, & \sigma^{\text{eff}} \geq 0. \end{cases} \quad (4)$$

For the reverse stress path,

$$\alpha_y(\sigma_{yy}, H) = \begin{cases} \alpha_y(\sigma_{yy}^{\text{max}}, H)[1 - N(\sigma_{yy}, H)], & \sigma^{\text{eff}} < 0, \\ \alpha_y(\sigma_{yy}^{\text{max}}, H), & \sigma^{\text{eff}} > 0, \end{cases} \quad (5)$$

where σ_{yy}^{max} is the maximal stress value achieved in the course of the forward stress path.

The normal strain $\varepsilon_{yy}^{(xy)}$ parallel to the compressive force is

$$\varepsilon_{yy}^{(xy)} = -(S^{-1}/2)\sigma^{\text{eff}}(\sigma_{yy}, H) + (c/a - 1) \times [\alpha_y(\sigma_{yy}, H) - \alpha_y(0, 0)], \quad (6)$$

where S is the elastic stiffness of detwinned martensite mechanically stressed in the y direction. (The state of the specimen at zero values of stress and field is taken as the undistorted one.) The term depending on the stiffness expresses the reversible part of the strain while the term involving the volume fraction is the irreversible part of the strain (for more detail see Ref. 17).

To be of any use, Eqs. (1), (2), and (4)–(6) require the function $\sigma^{\text{eff}}(\sigma_{ik}, H_j)$ to be known. The latter function can be deduced from the phenomenological magnetoelastic model of ferromagnetic martensite.^{13–15} According to this theory, the Gibbs energy density of a cubic crystal is expressed as (using SI units)

$$G = F_e - \delta M^2[\sqrt{3}(m_x^2 - m_y^2)u_2 + (2m_z^2 - m_y^2 - m_x^2)u_3] - \mathbf{m} \cdot \mathbf{H}\mu_0 M - (\sigma_2 u_2 + \sigma_3 u_3)/6, \quad (7)$$

where the term F_e denotes a Helmholtz energy of the deformed crystal, the term proportional to the phenomenological magnetoelastic parameter δ is a magnetoelastic energy (M is the magnitude of the magnetization vector \mathbf{M} , and $\mathbf{m} = \mathbf{M}/M$ is a unit vector with components m_x , m_y , and m_z), the third term is the Zeeman energy describing an interaction between the magnetization and an external magnetic field \mathbf{H} , μ_0 is the free-space magnetic permeability, and the last term is caused by the mechanical stressing of the crystal. The parameter δ is defined in Refs. 15 and 16 and has units of

MPa/T². The variables u_2 , u_3 , σ_2 , and σ_3 are linear combinations of the diagonal strain (ε_{ii}) and stress (σ_{ii}) tensor components,

$$u_2 = \sqrt{3}(\varepsilon_{xx} - \varepsilon_{yy}), \quad u_3 = 2\varepsilon_{zz} - \varepsilon_{yy} - \varepsilon_{xx}, \\ \sigma_2 = \sqrt{3}(\sigma_{xx} - \sigma_{yy}), \quad \sigma_3 = 2\sigma_{xx} - \sigma_{yy} - \sigma_{zz}, \quad (8)$$

where the coordinate axes x , y , and z are oriented in the [100], [010], and [001] directions, respectively. The σ_{ii} value is positive for a tensile and negative for a compressive stress along the i axis.

In the ferromagnetic parent phase (austenite), the strains u_2 and u_3 are caused by magnetostriction. In the ferromagnetic martensitic phase, spontaneous strains u_2^M and u_3^M arise, and therefore, the Gibbs energy of this phase can be obtained from Eq. (7) by the substitution $u_{2,3} \rightarrow u_{2,3}^M + u_{2,3}$. For the cubic-to-tetragonal martensitic transformation, $u_{2,3}^M \propto 1 - c/a$, and the substitution yields a magnetic anisotropy energy

$$w_A = 6\delta M^2(1 - c/a)m_i^2 \quad (9)$$

of the i variant of martensite, and a spontaneous magnetoelastic stress of the specimen is characterized by the functions

$$\sigma_2^{\text{me}} = 6\sqrt{3}\delta M^2(m_x^2 - m_y^2), \\ \sigma_3^{\text{me}} = 6\delta M^2(2m_z^2 - m_y^2 - m_x^2) \quad (10)$$

(for more details see the Appendix and Refs. 13–15). The rotation of the magnetization vector under the action of an external magnetic field is accompanied by the appearance of field-induced stresses or magnetostresses^{4,13}

$$\sigma_{2,3}(H) = \sigma_{2,3}^{\text{me}}(H) - \sigma_{2,3}^{\text{me}}(0). \quad (11)$$

The stress σ_3 is invariant with respect to the permutation $x \leftrightarrow y$ and, therefore, cannot initiate any motion of the twin boundaries. By contrast, the stress σ_2 changes sign upon permutation $x \leftrightarrow y$ and, hence, removes the equivalence of the twin components.

If a static magnetic field $\mathbf{H} \parallel x$ is applied to the specimen consisting of a single xy domain, it is perpendicular to the easy magnetic axis $c \parallel y$ of the y variant of martensite and a field-induced stress

$$\sigma_2(H) = \begin{cases} 12\sqrt{3}\delta M^2 H^2 / H_S^2, & H < H_S, \\ 12\sqrt{3}\delta M^2, & H \geq H_S, \end{cases} \quad (12)$$

arises owing to the rotation of the magnetization vector in the magnetic field. The value $H_S = 12|\delta(1-c/a)|M$ is the magnetic saturation field for the martensitic phase. The magnetic moment of the x variant is aligned along the x axis and, therefore, cannot be rotated by the magnetic field $\mathbf{H}\parallel x$. Therefore, $\sigma_2(H) = 0$ for the x variant, and thus, the effective field-induced stress is

$$\sigma^{\text{eff}}(H) = \sigma_2(H)/\sqrt{3}. \quad (13)$$

If $\delta < 0$, the stress $\sigma_2(H)$ is negative, and hence, this is the case of the field-induced compression of the specimen in the x direction or tension in the y direction [see statement (i) and Eq. (8)].

If a compressive stress $\sigma_{yy} < 0$ is applied to the specimen consisting of a single xy domain, the y variant of the martensite is compressed along the c axis while the x variant is compressed perpendicular to the c axis. The compression of the x variant with stress σ_{yy} is equivalent to its elongation under stress $\sigma_{xx} = -\sigma_{yy}$ because either stress results in the same σ_2 value. Therefore, the effective stress violating the equivalence of the martensite variants and initiating the twin boundaries motion is

$$\sigma^{\text{eff}} \equiv \sigma_{xx} - \sigma_{yy} = \sigma_2/\sqrt{3} = -2\sigma_{yy}. \quad (14)$$

When the magnetic field $\mathbf{H}\parallel x$ and stress σ_{yy} are applied to the specimen simultaneously, the effective stress is the sum of the values (13) and (14)—i.e.,

$$\sigma^{\text{eff}}(\sigma_{yy}, H) = \sigma_2(H)/\sqrt{3} - 2\sigma_{yy}. \quad (15)$$

The function (15) differs from the effective stress introduced in Ref. 17 by the factor of 2 in front of the σ_{yy} value. This difference is immaterial when the specimen is affected only by the magnetic field or only by the mechanical stress [in the latter case it results only in a redefinition of the parameters of the statistical distribution, Eq. (1)]. In contrast, the presence of the factor of 2 in Eq. (15) is essential for the determination of the equivalent field-induced stress, when both magnetic field and mechanical stress are applied to the specimen.

It can be summarized that the factor of 2 in Eq. (15) results from the fact that the mechanical stress affects both variants forming an xy domain, while the magnetic field $\mathbf{H}\parallel x$ stresses only one of them because the magnetic field rotates only the magnetization vector of the y variant.¹⁷ Moreover, it should be emphasized that according to Eqs. (1) and (14), the average mechanical stress needed for the reorientation of martensite is equal to $\sigma_c/2$, because in this case the effective stress is equal to σ_c . Nevertheless, the σ_c value is an adequate characteristic of the pinning energy of twin boundaries.

Equation (6) describes the deformation of martensite consisting of a single xy domain. The polydomain martensitic structure of the NMG2 specimen⁸ may be modeled by a mixture of xy , zy , and zx domains. The volume fractions of twin components in a zy domain depend on y and/or z components of the field, both being equal to zero in the case under consideration. Therefore, the deformation of a zy domain is

$$\varepsilon_{yy}^{(zy)} = -(S^{-1}/2)\sigma^{\text{eff}}(\sigma_{yy}, H) + (c/a)[\alpha_y(\sigma_{yy}, 0) - \alpha_y(0, 0)]. \quad (16)$$

For a zx domain, the strain component ε_{yy} is independent of the volume fractions of the twin components α_x and α_z . Therefore, the deformation of this domain is

$$\varepsilon_{yy}^{(zx)} = -(S^{-1}/2)\sigma^{\text{eff}}(\sigma_{yy}, H). \quad (17)$$

The average deformation for a mixture of the different twin structures is

$$\varepsilon_{yy} = \beta^{(xy)}\varepsilon_{yy}^{(xy)} + \beta^{(zy)}\varepsilon_{yy}^{(zy)} + \beta^{(zx)}\varepsilon_{yy}^{(zx)}, \quad (18)$$

where $\beta^{(ij)}$ denotes the volume fraction of ij domains in the experimental specimen.

It should be emphasized that Eq. (18) provides only the simplest approach to the problem, disregarding the elastic interaction between the spatial domains of martensite occupied by twins belonging to different domains (i.e., the internal stresses of the martensite are neglected).

IV. APPLICATION TO EXPERIMENTAL RESULTS

From fits of theoretical stress-strain curves calculated from the model equations [Eqs. (6) and (15)] for a series of $\sigma(H)$ values to the experimental stress-strain loops obtained by mechanical cycling of the specimen in stationary magnetic fields, the magnetic-field-induced stress can be obtained. Experimentally, the value

$$\sigma_{yy}^{\text{eq}} = \sigma_2(H)/2\sqrt{3} \quad (19)$$

is most indicative, because this value is equal to the mechanical stress needed for the compensation of stress induced by the magnetic field on the martensitic structure [see Eq. (15)]. Thus, the value σ_{yy}^{eq} can be referred to as the equivalent stress.

Figure 2 shows some of the experimental stress-strain loops obtained for NMG1 together with the fitted theoretical curves and σ_{yy}^{eq} values providing the best fit (the values $c/a = 0.94$, $\sigma_c = 3.0$ MPa, and $\sigma_0 = 0.75$ MPa were used). The field dependence of the equivalent stress obtained from the fitting procedure is shown in Fig. 3 together with $\alpha_y(H)$ and $\sigma_{yy}^{\text{eq}}(H)$ calculated from Eqs. (4), (12), and (19). The curve $\sigma_{yy}^{\text{eq}}(H)$ was calculated using a magnetization value $M = 0.6$ T and $\delta = -1.5$ MPa/T² for the magnetoelastic constant estimated from the magnetostriction of the austenitic phase^{5,15} and resulting in a reasonable theoretical value $\mu_0 H_S \approx 0.8$ T for the saturation field.

Figure 3 demonstrates satisfactory agreement between the field dependence of the equivalent stress extracted from the experimental stress-strain curves and quadratic dependence on magnetic field strength inherent to the magnetoelastic model in the field range $0 < \mu_0 H < 500$ mT. The maximal “experimental” value $\sigma_{yy}^{\text{eq}} \approx 3$ MPa is close to the value $\sigma_2(H_S)/2\sqrt{3} = 3.45$ MPa resulting from Eq. (12).

For comparison of the “experimental” values of the equivalent stress with the experimental $M(H)$ dependence (Fig. 4) measured for the different specimens of the NMG1 alloy, σ_{yy}^{eq} values are plotted in Fig. 5 together with

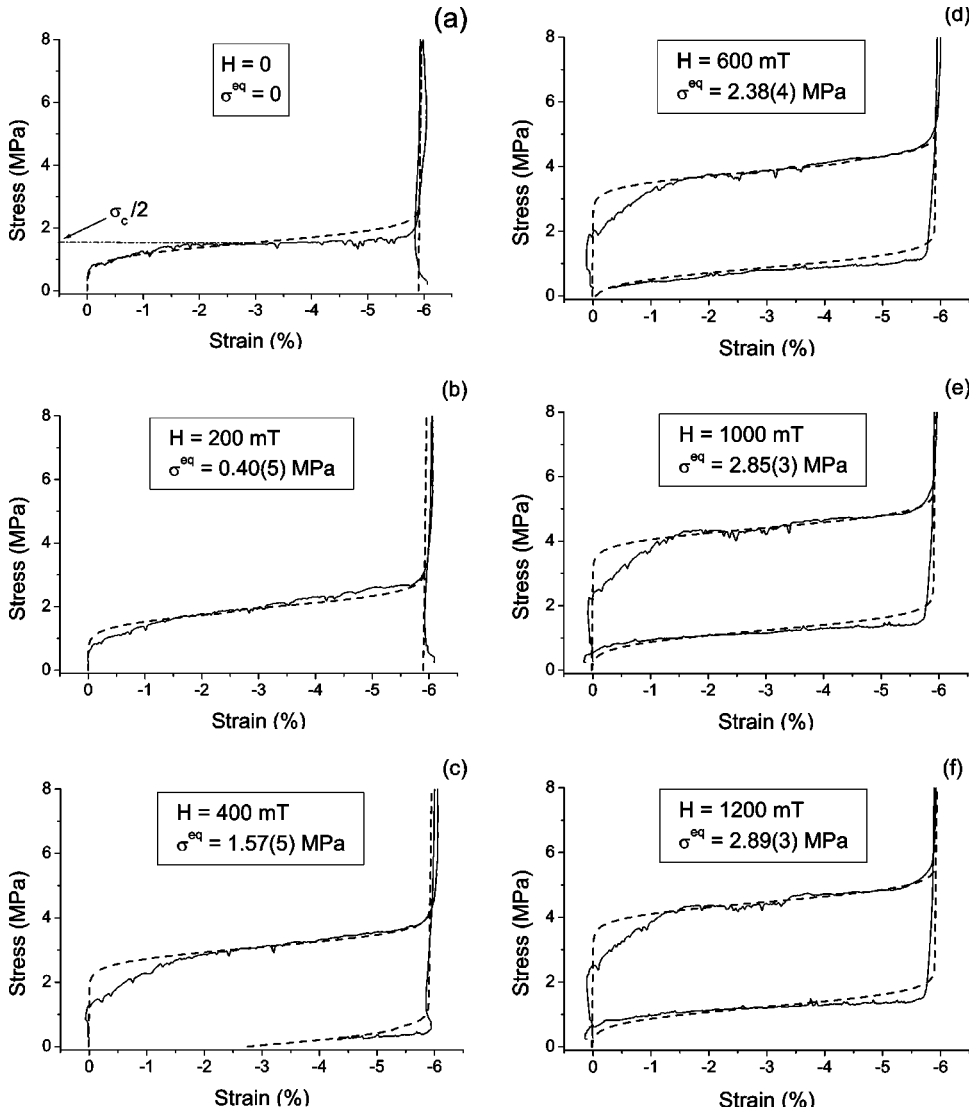


FIG. 2. A series of experimental (solid line) and theoretical (dashed line) stress-strain loops obtained at different constant fields for the single-crystalline NMG1 specimen consisting of a single martensitic xy domain. Compression stress is applied along $[010]$ while $H \parallel [100]$. The values of the magnetic field and experimentally determined equivalent stress are indicated on the graphs.

$\xi M^2(H/H_S)$ obtained from the experimental $M(H)$ dependence (a constant scaling factor $\xi = 8 \text{ MPa/T}^2$ was used) as functions of the reduced magnetic field H/H_S and the square $(M/M_S)^2$ of the reduced magnetization. Figure 5 demonstrates clearly the direct proportionality between the equivalent stress and the square of the magnetization and, therefore, the magnetoelastic nature of the magnetostrain effect in martensite [see Eq. (10)]. It becomes clear that the observed field dependence of the equivalent stress is not exactly quadratic for fields larger than ca. 500 mT (in Fig. 3 indicated by vertical dotted line) because for this field range the field dependence of the magnetization is not linear (see Fig. 4).

A precise adjustment of the theoretical stress-strain dependences to the experimental curves obtained for the NMG2 alloy is not possible in view of the complicated twin microstructure of the martensite in this specimen, but nevertheless, its magnetomechanical behavior can be understood taking into account the following features of the experimental stress-strain curves (Fig. 6):

(i) The maximal strain resulting from the reorientation of martensite variants under the effect of mechanical stress is about 2%.

- (ii) The maximal strain weakly depends on the strength of the applied magnetic field.
- (iii) Some reversible deformation is observed even in the absence of any magnetic field.

Feature (i) indicates that xy , xz , and yz domains occupy approximately equal volumes of the specimen (i.e., $\beta^{(xy)} = \beta^{(xz)} = \beta^{(yz)} = 1/3$) and the initial volumes of twin components are approximately equal to each other [i.e., $\alpha_x(0,0) = \alpha_y(0,0) = \alpha_z(0,0) = 1/2$].

Feature (ii) results from the statistical model when the parameter $|\sigma_c|$ appreciably exceeds the maximal value of the field-induced stress.

Feature (iii) shows that the martensitic state of the specimen is internally stressed. As the analytical form of the internal stress is not clear, this feature cannot be described in the framework of the statistical model in its present state.

Figure 6 shows experimental and theoretical stress-strain loops obtained for the martensitic alloy NMG2. The values of equivalent field-induced stresses were taken equal to those determined above for NMG1 martensite. In accordance with the features listed above, the parameters $\beta^{(ij)} = 1/3$, $\alpha_i(0,0)$

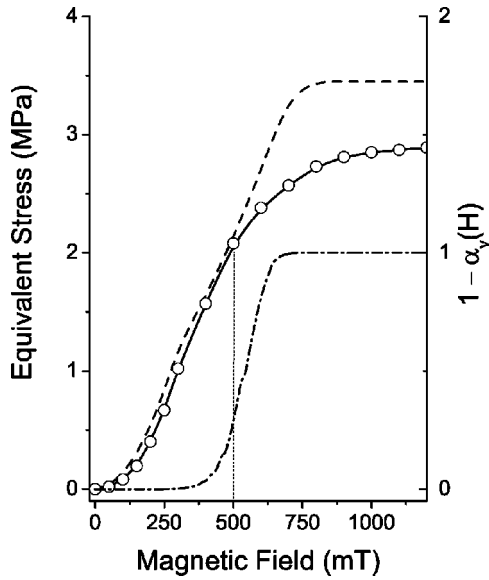


FIG. 3. Field dependence of the equivalent stress for single-crystalline NMG1 martensite determined theoretically by the described fitting procedure (solid line) and experimentally from the stress-strain data (open circles) in comparison with the quadratic function resulting from the magnetoelastic model (dashed line). The volume fraction of x variant in the xy domain is shown for illustration (dash-dotted line).

$= 1/2$, $|\sigma_c| = 4$ MPa, and $\sigma_0 = 1.1$ MPa were taken for the theoretical curves. The calculated dependences reasonably illustrate an evolution of the stress-strain loops accompanying variation of the magnetic field. A comparison of the experimental loops with the theoretical dependences clearly indicates the presence of internal stresses opposing the applied stress; the reversible part of the deformation observed experimentally exceeds the calculated reversible deformation for all field values.

The close fit of the model to experiments (Figs. 3 and 5) supports the statistical approach to twin boundary motion. It remains to find the micromechanistic origin of the statistical nature of the critical stress [assumption (iv) of the model]. On the microscopic scale, twin boundaries move by the motion of twinning dislocations.^{19,20} The magnetic field and the

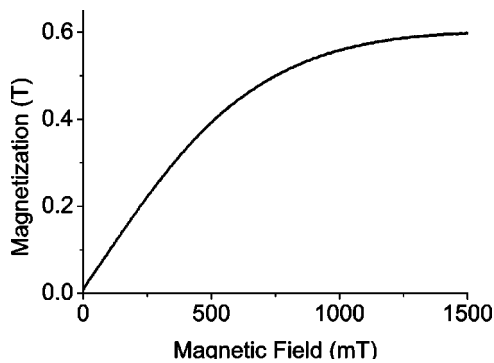


FIG. 4. Experimental magnetization curve taken in a magnetic field parallel to the shortest edge of the VSM specimen of the NMG1 alloy.

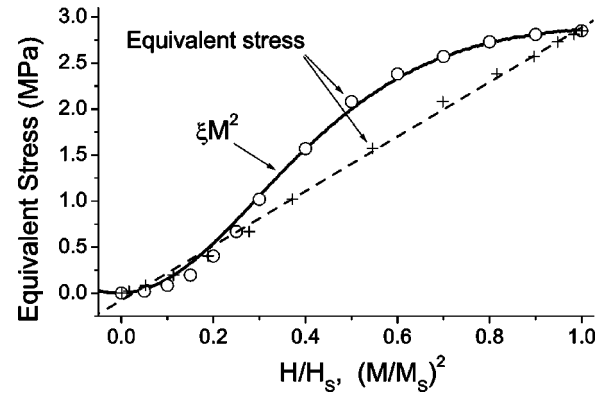


FIG. 5. The equivalent stress σ_{yy}^{eq} (circles) and square of magnetization ξM^2 (solid line) as a function of the reduced field H/H_S for NMG1 martensite. The equivalent stress is also presented as a function of the square of the reduced magnetization $(M/M_S)^2$ ($M_S = 0.6$ T): experiment (crosses) and linear fit (dashed line).

applied mechanical load exert magnetic and mechanical forces on a twinning dislocation.^{4,10} The magnetic force is the origin of the magnetic-field-induced stress.⁴ Dislocations themselves are sources of internal stresses which give rise to dislocation-dislocation interactions. The force on a twinning dislocation that results from the surrounding dislocations strongly depends on the dislocation structure—i.e., the spatial distribution of dislocations. The net force on the dislocation controls, on the microscopic scale, the onset and direction of dislocation motion and, on the macroscopic scale, the onset and direction of deformation.¹⁰ Since one of the contributions to the net forces—namely, that which results from dislocation-dislocation interaction—is spatially inhomogeneous, the critical contribution of the remaining magnetic (resulting from the applied magnetic field) and mechanical (resulting from the applied mechanical stress) forces is spatially inhomogeneous, too. This critical contribution to the net force on the twinning dislocation is reflected on the macroscopic scale by the critical stress for the boundary motion. Thus, the statistical nature of the dislocation structure directly results in the statistical distribution of σ^{eff} . As the density of twinning dislocations is larger in a polyvariant crystal than in a single-variant crystal, the width of the distribution of internal stresses (and thus σ_0) is expected to be larger in a polyvariant crystal than in a single-variant crystal. This again is in agreement with the results for NMG1 and NMG2.

V. DISCUSSION AND CONCLUSIONS

The present experimental and theoretical studies of the superelastic behavior of Ni-Mn-Ga martensite in a constant applied magnetic field have led to a consistent model described in this paper. In this model, magnetoelastic stress is responsible for both ordinary magnetostriction and detwinning of the microstructure. During detwinning, the magnetoelastic stress performs a mechanical work $w \propto 6 \delta M^2 (1 - c/a)$ per surface unit of the jumping interface. The present work shows that ordinary magnetostriction seems to be sufficient to trigger the detwinning of the specimen. This conclusion is supported, e.g., by the data of the mechanical

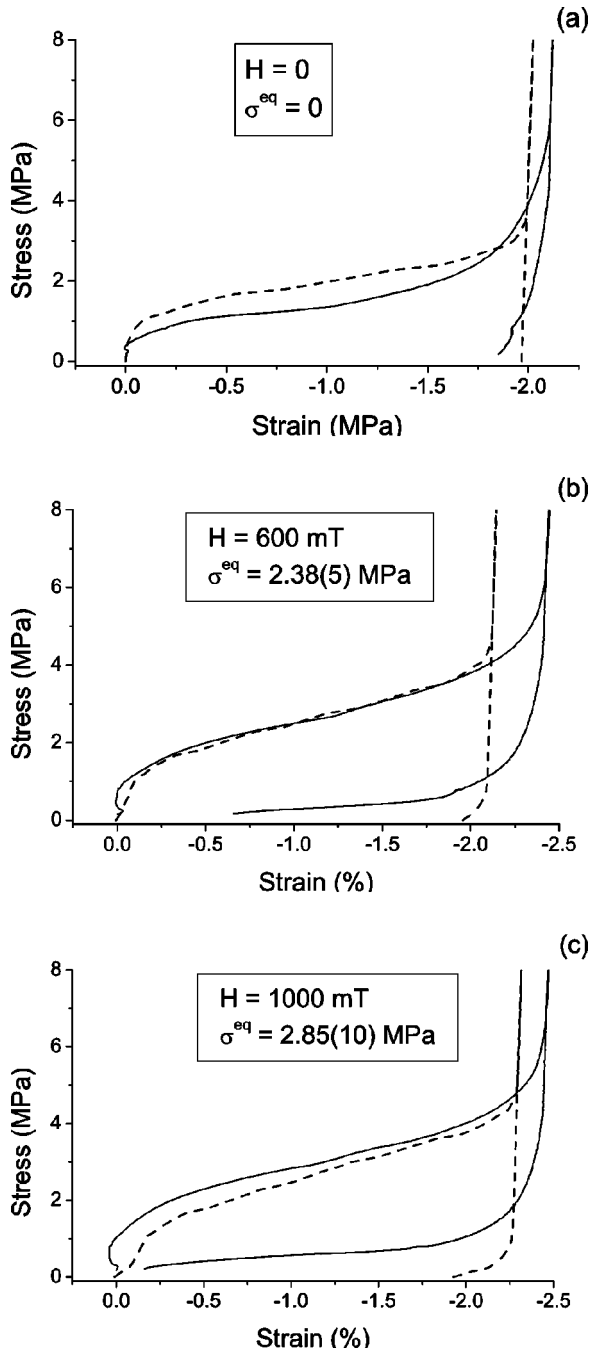


FIG. 6. A series of experimental (solid line) and theoretical (dashed line) stress-strain loops obtained for the NMG2 single crystal.

stress-strain test presented in Fig. 2(a). This figure demonstrates that during unloading, the detwinned martensite deforms linearly. From the slope of the stress-strain curve, an elastic compliance of $1.1 \times 10^{-4} \text{ MPa}^{-1}$ is obtained. This means that a stress of 1.8 MPa, causing complete detwinning of the martensite, induces a comparatively small elastic strain $\varepsilon^{(el)} \approx 2 \times 10^{-4}$. According to Ref. 21, this deformation exceeds the sustainable misfit for the different variants of a tetragonal lattice and results in the spatial rearrangement of twins. The ordinary magnetostriction measured in the austenitic phase of Ni-Mn-Ga alloy slightly exceeds the value

$\lambda = -10^{-4}$ (see Fig. 3 in Ref. 2) and is comparable to $\varepsilon^{(el)}$ (there is a tendency to magnetostriction increases on approaching the martensitic transformation temperature). Thus, one can conclude that the magnetostrictive deformation triggers the jumps of the twin boundaries and, hence, can be responsible for the detwinning of the martensite.

The statistical model presented here describes quantitatively the magnetic-field-induced superelastic behavior of the ferromagnetic martensite in Ni-Mn-Ga single crystals.

From a fit of theoretical stress-strain curves to the experimental ones, it becomes possible to determine the mechanical stress which is equivalent to the internal stress induced by the magnetic field. The experimental and theoretical results show that the field-induced stress is proportional to the square of the magnetization, supporting the theory that the magnetoelastic interaction is the fundamental source of the large strain caused by the field-driven twin rearrangement.

A comparison of theoretical stress-strain curves for the Ni-Mn-Ga single crystalline specimen containing differently twinned domains with experimental ones demonstrates the presence of internal stresses caused by the elastic interaction between the differently twinned spatial domains of martensite.

ACKNOWLEDGMENTS

V.A.C. is grateful to Japan Society for the Promotion of Science Grant No. RC30326005. The authors thank Dr. V. Khovailo for his help in magnetic measurements. P.M. and G.K. acknowledge partial support by the Swiss National Science Foundation (SNF).

APPENDIX

The Helmholtz energy of the cubic phase, involved in Eq. (7), is

$$F = \frac{1}{6} C' (u_2^2 + u_3^2) - \delta M^2 [\sqrt{3} (m_x^2 - m_y^2) u_2 + (2m_z^2 - m_y^2 - m_x^2) u_3], \quad (\text{A1})$$

where C' is the shear modulus. The substitution $u_{2,3} \rightarrow u_{2,3}^M + u_{2,3}$ with $u_{2,3}^M \propto 1 - c/a$ results in

$$F = \frac{1}{6} C' (u_2^2 + u_3^2) + 6 \delta M^2 (1 - c/a) m_i^2 - \delta M^2 [\sqrt{3} (m_x^2 - m_y^2) u_2 + (2m_z^2 - m_y^2 - m_x^2) u_3], \quad (\text{A2})$$

for the i variant of the tetragonal phase, corresponding to the linear approximation for a small parameter $1 - c/a$. In this approximation, the magnetic anisotropy energy corresponds to the tetragonal symmetry, while the elastic and magnetoelastic energies of the tetragonal phase coincide with those of the parent (cubic) phase. The “tetragonal corrections” to the elastic and magnetoelastic energies are proportional to $(1 - c/a)^2$ and are disregarded.

Using

$$\sigma_{ik} = (\partial F / \partial \varepsilon_{ik})_T, \quad (\text{A3})$$

we define σ_{ik} in terms of $u_{2,3}$:

$$\sigma_{2,3} = (\partial F / \partial u_{2,3})_T. \quad (\text{A4})$$

Equations (A2) and (A4) result in

$$\begin{aligned} \sigma_2 + 6\delta\sqrt{3}M^2(m_x^2 - m_y^2) &= 2C'u_2, \\ \sigma_3 + 6\delta M^2(2m_z^2 - m_y^2 - m_x^2) &= 2C'u_3, \end{aligned} \quad (\text{A5})$$

expressing Hooke's law for a stressed ferromagnetic crystal [cf. Eq. (10)].

Equations (A5) show that the magnetoelastic coupling is responsible for the occurrence of a stress $\sigma^{\text{me}} \sim \delta M_i^2$, which is quadratic in the components of the magnetization vector \mathbf{M} . Purely magnetic terms in a free energy cannot contribute to the mechanical stress because they are independent of the strain tensor components.

*Author to whom correspondence should be addressed. Electronic address: t.takagi@ieee.org

¹V. A. Chernenko, E. Cesari, V. V. Kokorin, and I. N. Vitenko, *Scr. Metall. Mater.* **33**, 1239 (1995).

²K. Ullakko, J. K. Huang, C. Kantner, R. C. O'Handley, and V. V. Kokorin, *Appl. Phys. Lett.* **69**, 1966 (1996).

³R. C. O'Handley, S. J. Murray, M. Marioni, H. Nembach, and M. S. Allen, *J. Appl. Phys.* **87**, 4712 (2000).

⁴P. Müllner, V. A. Chernenko, M. Wollgarten, and G. Kostorz, *J. Appl. Phys.* **92**, 6708 (2002).

⁵V. A. L'vov, E. V. Gomonaj, and V. A. Chernenko, *J. Phys.: Condens. Matter* **10**, 4587 (1998).

⁶A. Sozinov, A. A. Likhachev, N. Lanska, and K. Ullakko, *Appl. Phys. Lett.* **80**, 1746 (2002).

⁷C. Jiang, T. Liang, H. Xua, M. Zhang, and G. Wu, *Appl. Phys. Lett.* **81**, 2818 (2002).

⁸P. Müllner, V. A. Chernenko, and G. Kostorz, *Scr. Mater.* **49**, 129 (2003).

⁹M. Pasquale, C. P. Sasso, S. Besseghini, and V. A. Chernenko, *IEEE Trans. Magn.* **37**, 2669 (2001).

¹⁰P. Müllner, V. A. Chernenko, and G. Kostorz, *J. Magn. Magn. Mater.* **267**, 325 (2003).

¹¹R. C. O'Handley, *J. Appl. Phys.* **83**, 3263 (1998).

¹²R. D. James and M. Wuttig, *Philos. Mag. A* **77**, 1273 (1998).

¹³V. A. Chernenko, V. A. L'vov, and E. Cesari, *J. Magn. Magn. Mater.* **196-197**, 859 (1999).

¹⁴V. A. Chernenko, V. A. L'vov, E. Cesari, and P. McCormick, *Mater. Trans., JIM* **41**, 928 (2000).

¹⁵V. L'vov, S. Zagorodnyuk, V. Chernenko, and T. Takagi, *Mater. Trans., JIM* **43**, 876 (2002).

¹⁶M. Pasquale, C. P. Sasso, G. Bertotti, V. A. L'vov, V. A. Chernenko, and A. De Simone, *J. Appl. Phys.* **93**, 8641 (2003).

¹⁷N. I. Glavatska, A. A. Rudenko, I. N. Glavatskiy, and V. A. L'vov, *J. Magn. Magn. Mater.* **265**, 142 (2003).

¹⁸V. A. Chernenko, V. A. L'vov, S. P. Zagorodnyuk, and T. Takagi, *Phys. Rev. B* **67**, 064407 (2003).

¹⁹J. W. Christian and S. Mahajan, *Prog. Mater. Sci. Eng.* **39**, 1 (1995).

²⁰P. Müllner and W. M. Kriven, *J. Mater. Res.* **12**, 1771 (1997).

²¹D. S. Lieberman, T. A. Read, and M. S. Wechsler, *J. Appl. Phys.* **28**, 532 (1957).